Global electronic structure of semiconductor alloys through direct large-scale computations for III-V alloys $Ga_xIn_{1-x}P$

Yong Zhang[1] and Lin-Wang Wang[2]
[1]*Department of Electrical and Computer Engineering and Center for Optoelectronics, University of North Carolina at Charlotte, Charlotte, North Carolina 28223, USA*
[2]*Lawrence Berkeley National Laboratory, Berkeley, California 94720, USA*
(Received 9 February 2011; revised manuscript received 3 March 2011; published 26 April 2011)

We critically examine two nominally equivalent approaches for treating a random alloy: (1) by using one very large supercell as a direct simulation of the alloy and (2) by performing configuration averaging over many smaller supercells; and the common practice using a virtual crystal as the reference for analyzing the alloy band structure and discussing the electronic transport in the alloy. Specifically, (1) we show that, in practice, the size of the "very large" supercell depends on the particular property of interest, and the ideal of configuration averaging is only useful for certain properties. (2) We also examine the assumed equivalency by comparing the results of the two approaches in band-gap energy, energy fluctuation, and intervalley and intravalley scattering, and conclude that the two approaches often lead to nonequivalent physics. (3) We use a generalized moment method that is capable of computing the global electronic structure of a sufficiently large supercell (e.g., ∼260 000 atoms) to obtain the intrinsic broadening of a Γ-like electron state caused by the "inelastic" intravalley scattering in a direct-band-gap semiconductor alloy. (4) We demonstrate an efficient way to construct the effective dispersion curves of the alloy with high accuracy for calculating effective masses and examining anisotropy and nonparabolicity of the dispersion curve. (5) Finally, we discuss the limitation of using the virtual-crystal approximation as the reference for evaluating alloy scattering and studying transport properties.

DOI: 10.1103/PhysRevB.83.165208 PACS number(s): 71.23.An, 71.15.Dx, 72.20.Dp, 71.20.Nr

I. INTRODUCTION

Disordered alloys have been traditionally treated by approximate methods such as the virtual-crystal approximation (VCA) or coherent-potential approximation (CPA).[1,2] However, there could be serious omissions in such approximate methods. In VCA, for an alloy $A_xB_{1-x}C$, the potentials of the A and B substitutional atoms are averaged to yield a simple periodic system over the primitive unit cell. In CPA, the energy-dependent transfer matrix (t matrix) of atoms A and B is averaged. Correspondingly, an energy-dependent coherent potential is introduced in the Hamiltonian, which again makes the potential periodic over the primitive unit cell, albeit the resulting Hamiltonian is non-Hermitian. This periodic but non-Hermitian Hamiltonian gives us a band structure with a finite width for each band state. However, the multiple scatterings between A and B have been ignored in such a treatment.

To include all the scattering effects in a straightforward manner, another approach is to calculate directly a finite disordered system. One such method is the special quasirandom structure (SQS) method,[3] where a relatively small superlattice system is constructed to have the atom-atom correlation functions as close as possible to those in a true random system. But the SQS method has a major limitation; namely, a SQS has a well-defined symmetry that has undesirable physical consequences (for instance, the splitting of the valence band that is supposed to be degenerate for a random alloy). With increasing computing power, it has become possible to use very large supercells to represent a true random alloy. However, in the past, the use of a very large supercell (on the order of one million atoms), with the help of a folded-spectrum method, typically allowed the calculation of only a few states near a selected energy level, such as the conduction band minimum or valance band maximum.[4]

As demonstrated in the current paper, with the help of a more efficient computational technique, we can now use a supercell containing a quarter-million atoms (or more) to study the electronic structure of an alloy for practically any required spectral range. This opens up a different avenue to investigate the electronic structure of either totally random or partially ordered alloys. In random systems, fluctuation and statistical averaging become the essential theme. The fluctuation in a finite-size system, which is only available in the supercell approach, can in principle provide information that can be compared directly with the result of optical spectroscopy. In this paper, we will discuss the different statistical approaches and the meanings of the differently averaged results. We will also show how the supercell approach can yield the alloy band structure and band width, and how they are related to the CPA band structure and the roles of intervalley and intraband scattering when using the VCA as a reference.

By definition, an alloy does not have translational symmetry. In principle, we need to deal with a quantum mechanical system with a large number of atoms in any macroscopic device involving the alloy. For instance, a 100-nm cube contains >40 million atoms. If one is not constrained by the computational power, what would be the appropriate structure size to simulate the electronic structure of an alloy? Intuitively, two approaches can be used to solve the quantum mechanical problem of the alloy:[1] (1) constructing and solving one single sufficiently large structure as representative for the alloy, or (2) constructing many relatively small-size structures (but still containing many atoms, much larger than any typical SQS), then solving them individually followed by configuration averaging.

It is generally believed that these two approaches should in principle lead to the same results if the "small" size

system is sufficiently large, because a macroscopically large crystal may be visualized as composed of many smaller but different pieces.[1] However, such equivalency has never been rigorously examined. Even though the CPA theory is generally formulated based on configuration averaging,[1,2] because the single-site approximation is typically used in a real calculation, the result becomes independent of the size and detail of the configurations. The supercell approach makes it feasible to directly test these two approaches. However, when actually implementing either approach, one will encounter a few practical issues. For instance, what structure size can be considered as "sufficiently large" to be representative for the alloy and what size is appropriate to be used as the "small structure" for the purpose of configuration averaging? If the size is too small, will the averaged result deviate from that of the infinitely large supercell result? Does the fluctuation of the finite-size results have any physical meaning? Perhaps the two most basic pieces of knowledge regarding the electronic structure of a semiconductor alloy are its fundamental band gap and inhomogeneous broadening. Therefore, in this work, we will examine the two approaches, focusing primarily on these two basic physical properties. We find that greatly different supercell sizes are required to address different alloy problems. For instance, one supercell size that is capable of yielding a satisfactory accuracy in the band gap might be totally inadequate or result in misleading information regarding alloy scattering. Thus, it is neither practical nor necessary to find one supercell size that suits all purposes. We will therefore discuss what the appropriate supercell size is for a particular property of interest.

First, the required supercell size depends on our convergence goal. A reasonable convergence goal for the electronic structure calculation of the semiconductor alloy is to achieve the accuracy obtainable by optical spectroscopy that is usually more accurate than other experimental techniques. For a semiconductor alloy that is well prepared and characterized (e.g., the composition is accurately known), the band gap E_g can be determined by optical spectroscopy with an accuracy of a few meV for a given composition x; for instance, for the prototype system $Ga_xIn_{1-x}P$ to be examined in this work.[5] A benchmark test has revealed that, for the alloy $Ga_xIn_{1-x}P$, the band gap converges to about 10 meV or about 1 meV by configuration averaging over 432-atom supercells or 3456-atom supercells, respectively, when comparing to the result of one 27 648-atom supercell.[6] In this work, by applying the more efficient generalized moment method (GMM), we are able to calculate an even larger supercell with 259 200 atoms and further confirm the convergence of the configuration average of the 3456-atom supercell for the band-gap energy.

Note that the use of the GMM does not affect the convergence of a particular material property with respect to the supercell size but does affect the efficiency to reach the desirable accuracy. Therefore, for the purpose of calculating the alloy band gap, we have established a guideline for the supercell size for the two approaches: 3000–4000 atoms for doing the configuration averaging or around 30 000 atoms for using one representative configuration. Although this guideline is based on $Ga_xIn_{1-x}P$, it is likely valid for most conventional semiconductor alloys. For a linear scaling method like the GMM or the folded-spectrum method, the fact that the supercell size differs by a factor less than 10 for the two approaches suggests that the configuration-averaging approach does not necessarily require less computational effort, considering the need to calculate many configurations (typically 50–100 configurations) for a small system to provide good statistics.

Second, the required supercell size depends on the specific alloy property to be studied. For instance, to investigate the intrinsic spectral broadening of a band-edge alloy state, the approach of using one very large supercell is necessary, although the statistical fluctuation of many smaller structures might have its own physical significance.

In the supercell simulation of the alloy, a practical issue is the selection of a boundary condition. There are three possible boundary conditions that can be applied in the calculation: (1) periodic repetition of the supercell, (2) an isolated supercell in vacuum, and (3) periodic repetition but with barriers inserted between the alloy structures. Unfortunately, none of these are a perfect choice. Option (1) will lead to coupling among supercell units, option (2) leads to coupling between surface states, whereas option (3) leads to coupling between the alloy and barrier material. Option (1) is the easiest to implement, and one may hope that, with the use of a sufficiently large supercell, the intersupercell coupling becomes negligible. There is another potential advantage of choosing (1), that is, the periodic system allows the use of $\mathbf{k}$ points (although in a very small Brillouin zone for a large supercell). As we will see later, the dispersion of the supercell can be connected with the alloy band structure in a seamless fashion for a large supercell.

One can compute directly a number of electronic and optical properties such as band gap, density of states, and dielectric functions for a semiconductor alloy without having to introduce a reference Hamiltonian. However, to understand the spectral broadening due to the alloy fluctuation and closely related transport properties, it is useful to introduce a reference Hamiltonian, typically the VCA, to provide the reference states free of alloy scatterings.[1,2] A spectral function $A_n(\mathbf{k},\mathrm{E})$ can be defined as

$$A_n(\mathbf{k},E)=\sum_i |\langle\psi_i|\phi_{n,\mathbf{k}}\rangle|^2\delta(E-\varepsilon_i), \tag{1}$$

where ψ_i is the alloy eigenstate with energy ε_i, and ϕ_{nk} is the VCA wave function at a $\mathbf{k}$ point of the primary-cell Brillouin zone (BZ) with a band index n. This spectral function describes how a VCA state is decomposed into different alloy states. In a way it is a $\mathbf{k}$-resolved density of states of the alloy. If the alloy fluctuation does not introduce any coupling among the VCA states, the spectral function would be a single δ function at energy $E=E(\mathbf{k})$ for a given $\mathbf{k}$. For a disordered system, the finite width of $A(\mathbf{k},E)$ can be related to the quasiparticle life time. It is very similar to the finite-energy width in the CPA theory, and also related to the scattering rate based on the VCA treatment. The spectral width for a general $\mathbf{k}$ point of the VCA band structure, high-symmetry points of the BZ in particular, will be an important topic to be discussed in this paper. Note that, in the direct supercell calculation, the spectral width can include both elastic coupling (among degenerate $\mathbf{k}$ points) and inelastic coupling (among nondegenerate $\mathbf{k}$ points). In most CPA and VCA treatments, only elastic coupling is considered, although second-order perturbation theory involving nondegenerate states is used to

explain the band-gap bowing effect based on the VCA. As a result, the spectral width is simply proportional to $\rho(E)$, which is the density of states of the unperturbed reference system (e.g., the VCA system). We will show that, in the full supercell treatment, this is not generally true.

A number of semiconductor alloys have been previously investigated for their spectral functions $A(\mathbf{k},E)$. For III-V alloys with relatively small lattice and chemistry mismatches, such as $Al_xGa_{1-x}As$ and $Ga_xIn_{1-x}As$, $A(\mathbf{k},E)$ is found to be very sharp (practically a δ function) by using the CPA or molecular-CPA theory[7,8] in the direct-band-gap composition region at $\mathbf{k} = 0$ (the Γ point), because elastic intervalley scattering is not possible and inelastic intravalley scattering is very weak for the lowest conduction band state, which explains why electronic transport in a direct-band-gap alloy usually does not degrade drastically from a true crystalline structure. For the indirect-band-gap alloy Si_xGe_{1-x}, the spectral width of $A(\Gamma,E)$ was found to vary from 1 meV at $x = 0.1$ to 0.2 eV at $x = 0.5$. Because the alloy band gaps are indirect, the Γ-like state is in resonance with other $\mathbf{k}$ points that are degenerate with the Γ state, leading to significant intervalley coupling.[9] We have recently found that, by a direct calculation using the 27 648-atom supercell for $Ga_xIn_{1-x}P$ with $x = 0.8$ in the indirect-band-gap region the $A(\Gamma,E)$ spectrum barely shows a peak to allow for the identification of the Γ-like state in the alloy.[10] However, for $x = 0.5$ in the direct-band-gap region, the 27 648-atom supercell is far from adequate to reveal the intrinsic $A(\Gamma,E)$ spectrum because alloy scattering to the Γ state is very weak. Very recent extension of a similar analysis to the more strongly mismatched alloys $In_xGa_{1-x}N$, using the supercell method with a size up to about 4000 atoms[11] has yielded qualitatively the same observation as for other simpler alloys. By calculating $A(\mathbf{k},E)$ throughout the BZ, one can construct an effective band structure for an alloy using a properly defined VCA reference band structure, which has been done for numerous semiconductor alloys such as $Hg_{1-x}Cd_xTe$,[12] Si_xGe_{1-x},[9] $Ga_{0.5}In_{0.5}As$, $ZnSe_{0.5}Te_{0.5}$,[7] and the latest: $In_xGa_{1-x}N$.[11] It turns out that the most challenging task is to accurately calculate $A(\Gamma,E)$ for a direct-band-gap material, which has never been explicitly calculated using a sufficiently large supercell but is fundamentally important to understand the alloying effect.

In this work, we first introduce in Sec. II the generalized moment method that can evaluate the spectral function $A(\mathbf{k},E)$ far more efficiently than previously used approaches, particularly for very large supercells. In Sec. III, we apply this method to the prototype alloy system $Ga_xIn_{1-x}P$ to investigate the intravalley scattering of the Γ point or the inhomogeneous broadening of the single electron state (III-A) and to analyze the inter- and intravalley scattering at the L and X points and the alloy scattering-induced spectral broadening for the general alloy states far away from the band edge. We also construct the effective dispersion curves and calculate the effective masses of the alloy bands (III-B) for $x = 0.5$ in the direct-band-gap region and compare the spectral functions obtained by configuration averaging with moderate size supercells and one very large supercell for $x = 0.8$ in the indirect-band-gap region (III-C). Furthermore, in Sec. IV, we discuss the limitations of studying alloy scattering within the VCA framework. Finally, a summary is given in Sec. V.

II. THEORETICAL METHODS

We use in this work an empirical pseudopotential method (EPM),[13] which has been successfully applied to the study of the electronic structure of $Ga_xIn_{1-x}P$ alloys.[6,10] The (reciprocal-space) empirical pseudopotential takes the form of $v(q,\boldsymbol{\varepsilon}) = v(q,0)[1 + a_s\mathrm{Tr}(\boldsymbol{\varepsilon})]$, where $v(q,0)$ is the value for the equilibrium lattice constant, and $\mathrm{Tr}(\boldsymbol{\varepsilon})$ is the trace of the local strain (approximated by the relative change of the tetrahedron volume).[13] The extra term associated with the strain parameter a_s offers a significant improvement over the conventional EPM in the presence of strain and lattice relaxation. Because the pseudopotentials for the common P anion are fit separately for GaP and InP and are thus nonidentical, the P pseudopotential is taken as a weighted average in a combined system according to the number of Ga and In atoms on the four nearest-neighbor cation sites to account for the difference in the local chemical environment.[13] The strain term is set to zero for the common anion P pseudopotentials. The pseudopotentials were obtained by fitting to experimentally determined or theoretically calculated electronic properties at their equilibrium conditions. These properties include energies, deformation potentials, effective masses at different critical points, and valence-band offsets. The pseudopotentials can reproduce very well not only the binary band structures, but also the alloy band structure in the whole composition range with varying degrees of order.[6,14] A plane-wave basis is used to expand the electronic wave function, with a kinetic-energy cutoff of 7 Ry.

In the supercell calculation, if all the alloy eigenstates $\{\psi_i\}$ need to be calculated to obtain the projection in Eq. (1), the calculation will be extremely expensive. In that case, one is either limited to analyze only a few special $\mathbf{k}$ points (Γ, X, L) while using a large supercell (e.g., ~30 000 atoms)[10,15] or forced to use smaller supercells (e.g., ~4000 atoms or below) to get the full dispersion curves.[11] For instance, in our previous effort studying the band structure of $Ga_xIn_{1-x}P$ with $x = 0.8$ using a 27 648-atom supercell, although the Γ-like state is located merely ~0.1 eV above the band edge, $A(\Gamma,E)$ spreads over a large spectral range. Thus, we had to calculate 200 states over a 230-meV spectral range for this large supercell.[15] Even with the use of a very efficient computational technique (i.e., the folded spectrum method[16]), which allowed us to compute only the states close to a selected reference energy, the computation effort was still a major undertaking. Furthermore, we had to analyze the projections of all 200 computed states to obtain the spectrum function $A(\Gamma,E)$ in the spectral window of interest, which is also time consuming.

Often, one cannot tell *a priori* where the peak of $A(\mathbf{k},E)$ should appear and how many states to calculate, if it is practically feasible to calculate the required number of states. In this work, we instead adopt the generalized moment method to calculate the spectral density function $A(\mathbf{k},E)$. In this method, we first generate the VCA state $\phi_n(\mathbf{k},\mathbf{r})$ within the primary cell, and then extend it over the whole supercell. Note that this procedure works for any arbitrary $\mathbf{k}$ point of the VCA BZ. If the $\mathbf{k}$ point is not folded to the Γ point of the supercell, then a corresponding $\mathbf{k}'$ point of the supercell cell BZ needs to be used. Assuming that the supercell Hamiltonian is H (which has been rescaled, so the

minimum and maximum eigenenergies are within [−1,1]), we can generate the following Chebyshev wave functions via a recursion method:[17]

$$\phi_1 = H\phi_o, \tag{2}$$

$$\phi_j = 2H\phi_{j-1} - \phi_{j-2} = T_j(H)\phi_0, \tag{3}$$

where $\phi_0 = \phi_{nk}$, and $T_j(x)$ is the Chebyshev polynomial. Now, we can construct the jth moment:

$$\begin{aligned} I_j &= \langle\phi_0|\phi_j\rangle \\ &= \langle\phi_{nk}|T_j(H)|\phi_{nk}\rangle = \sum_i \langle\phi_{nk}|\psi_i\rangle\langle\psi_i|T_j(H)|\phi_{nk}\rangle \\ &= \sum_i T_j(\varepsilon_i)|\langle\phi_{nk}|\psi_i\rangle|^2. \end{aligned} \tag{4}$$

Using the definition of Eq. (1), we have

$$I_j = \int_{-1}^{1} T_j(E)A_n(\boldsymbol{k},E)dE. \tag{5}$$

This is the Chebyshev moment of the spectral function $A_n(\mathbf{k},E)$. With many such moments (up to mth order), we can reconstruct the spectral function $A_n(\mathbf{k},E)$ as follows:

$$A_n(\boldsymbol{k},E) = \frac{2}{\pi}(1-E^2)^{-1/2}\sum_{j=0,m} T_j(E)I_j(1+\delta_{j,0}). \tag{6}$$

The size of m determines the energy resolution of $A_n(\mathbf{k},E)$. That m is a finite number leads to broadening of each of the δ functions in $A_n(\mathbf{k}, E)$ in Eq. (1) at $E = E_i$ into a Gaussian function:

$$f(E') = \exp\left[-\frac{(E'-E_i)^2}{\gamma^2}\right], \tag{7}$$

where $\gamma = 4m^{-1}(E_{\max} - E_{\min})\sqrt{1-[(E_{\max}-E')/(E_{\max}-E_{\min})]^2}$, and $E_{\max}$ and $E_{\min}$ are, respectively, the maximum and minimum energy of the full spectrum that the alloy states span. In the language of optical spectroscopy, the parameter γ determines the spectral resolution with a full width at half maximum (FWHM) given by $2\gamma\sqrt{\ln 2}$, and m determines the step size given by $\Delta = (E_{\max} - E_{\min})/m$, typically about FWHM/6. To resolve the alloy states of a large supercell, a large m is desirable. For calculating $A(\mathbf{k},E)$, we used $m = 200\,000$ (FWHM $\approx$ 2.3 meV) for 27 000-atom supercells, and $m = 300\,000$ (FWHM $\approx$ 1.5 meV) for the largest supercell of 259 200 atoms, in an attempt to obtain $A(\mathbf{\Gamma}, E)$ for the conduction-band band-edge state at $x = 0.5$. For large m, Eq. (6) can be carried out via a fast Fourier transform.[17] We note that, in this moment method, the numerical error is not amplified through the recursive application of the Hamiltonian, rather a simple accumulation occurs of the numerical errors from individual iterations. Even with the use of a large number of moments (e.g., $m =$ 300 000 or larger), because of the use of double precision, there is no problem with numerical stability and accuracy.

In the configuration-averaging approach, $A_n(\mathbf{k},E)$ can be obtained by averaging over many configurations:

$$\bar{A}_n(k,E) = \langle A_n(k,E)\rangle_{\text{config}}. \tag{8}$$

In this work, we use Eq. (1) for supercell sizes >27 000 atoms and Eq. (8) for 3456-atom supercells by averaging over 50 randomly generated configurations. In our previous work,[6,10,15] for convenience in studying the CuPt ordering, an orthorhombic supercell was adopted with three cell vectors $\mathbf{a}_1$, $\mathbf{a}_2$, and $\mathbf{a}_3$ along the $x' \sim [11\bar{2}]$, $y' \sim [\bar{1}10]$, and $z' \sim$ [111] direction of the zinc-blend (ZB) crystal, respectively. The supercell containing 27 648 atoms has $a_1 = 12a\sqrt{3/2}$, $a_2 = 12a\sqrt{2}$, and $a_3 = 8a\sqrt{3}$, where a is the lattice constant of the alloy that is assumed to follow Vegard's rule with $a_{\text{GaP}} = 5.447$ Å and $a_{\text{InP}} = 5.8658$ Å. Smaller supercells with a factor 2 and 4 reduction along all directions are also used with 3456 and 432 atoms, respectively. In this work, we also use two cubic supercells—one with $a_1 = a_2 = a_3 = 15a$ or 27 000 atoms and one with $a_1 = 144a$ and $a_2 = a_3 = 15a$ or 259 200 atoms. A valence force-field method is applied to relax all the atoms within the supercell to minimize the strain energy.[18] In the supercell, the total number of the cation atoms is enforced to satisfy the composition x, and they randomly occupy the corresponding sublattice. Virtual-crystal calculations are also performed, with the pseudopotential given by $v(q,\boldsymbol{\varepsilon}) = xv^{\text{GaP}}(q,\boldsymbol{\varepsilon}) + (1-x)v^{\text{InP}}(q,\boldsymbol{\varepsilon})$.

III. RESULTS AND DISCUSSION

A. Intrinsic broadening due to alloying

As pointed out in the introduction, for different purposes and convergence expectations, different supercell sizes are required. Figure 1 shows the histogram plots for the band gaps of disordered $Ga_{0.5}In_{0.5}P$ calculated using two supercell sizes: Fig. 1(a) for the 432-atom supercell and Fig. 1(b) for the 3456-atom supercell, each with 100 configurations. When the size increases from 432 atoms to 3456 atoms, not only does the energy fluctuation decrease, but the average band gap increases from 1.971 to 1.980 eV. The latter is very close to the result of one even larger supercell—27 648 atoms, 1.979 eV.[6] Therefore, for the purpose of determining the band gap, the configuration averaging using the 3456-atom supercell is considered adequate. The FWHM for the histogram plot of Fig. 1(b) is $\Delta_{\text{cf}} = 8.3$ meV,[19] which turns out to be similar to the excitonic linewidth $\Delta_{\text{ex}} = 8$ meV for this alloy measured by the excitonic emission at low temperature.[20] It is reasonable to expect some connection between Δ_{cf} and Δ_{ex}, but we will leave this aspect for future work. We only wish to point out here that Δ_{cf} is rather different from the most popularly considered mechanism for the excitonic linewidth in a semiconductor alloy where the width is caused by the energy variation as a result of composition fluctuation within the "exciton volume" from one area to the other.[21] In our case, the average composition within the supercell is kept the same and the band-gap fluctuation is purely due to the arrangement of the atoms in the microscopic scale. In this work, we instead focus on the difference between Δ_{cf} and the width of $A(\Gamma,E)$, the intrinsic broadening of the band-edge alloy state, to be investigated below. To determine $A(\Gamma,E)$, not only the 3456-atom cell but even the 27 648-atom cell is far from sufficient.

Figure 2(a) shows $A(\Gamma,E)$ for the conduction band minimum (CBM) calculated from one 3456-atom and one 27 648-atom supercell, with $A(\Gamma,\text{CBM}) = 0.867$ and 0.864, respectively. Although it appears the CBM has a large component of the

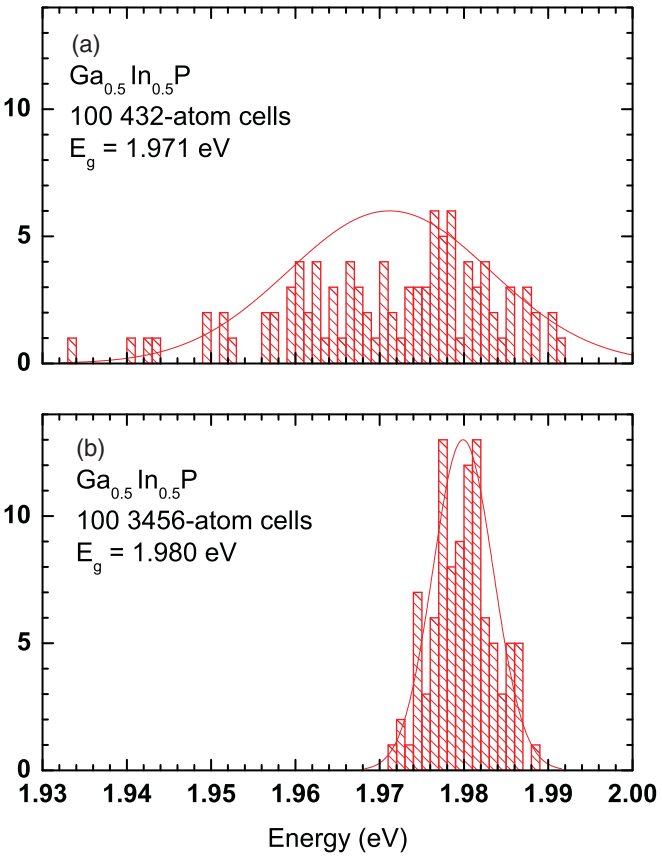

FIG. 1. (Color online) Histogram plots of the energy distributions of the band gap (E_g) for the $Ga_{0.5}In_{0.5}P$ alloy calculated using two super-cell sizes.

VCA Γ state, the results in fact represent the integrated VCA Γ components for all the alloy states within a spectral range of ∼20 or ∼145 meV, respectively, for the two supercell sizes. The range is roughly given by the energy separation between the band-edge state and the nearest alloy state, as shown in Fig. 2(a), depending on the size of the supercell.

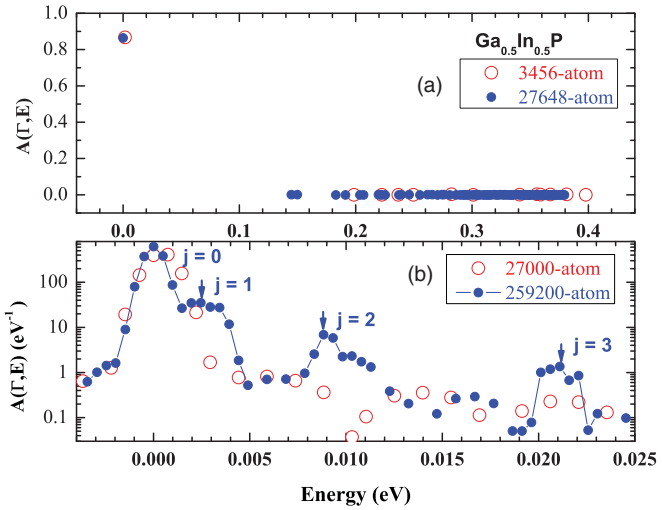

FIG. 2. (Color online) Spectral functions $A(\mathbf{k} = 0,E)$ near the conduction band minimum for the $Ga_{0.5}In_{0.5}P$ alloy (a) obtained by projecting the alloy wave functions onto the VCA state at $\mathbf{k} = 0$ and (b) calculated by applying the generalized moment method with the $\mathbf{k} = 0$ VCA state as the reference.

To be able to investigate the intrinsic broadening of the alloy CBM state in this direct-band-gap semiconductor, one would need to use an even much larger supercell. If we would like to examine the coupling of the CBM to other alloy states lying within 1–2 meV of the CBM, the supercell dimension needs to be increased by roughly a factor of 10, assuming the effective mass is in the order of $m^* \sim 0.1$. Therefore, we have tested two supercell sizes based on an 8-atom cubic cell with size 15×15×15 and 144×15×15, using the much more efficient GMM. The results are shown in Fig. 2(b). Note that, in Fig. 2(b), each peak represents one alloy state that has a nonzero projection onto the VCA CB Γ state and is broadened by the lineshape function of Eq. (7). Again, the 27 000-atom cell does not reveal any alloy state within the vicinity of the CBM, but the 259 200-atom cell does give rise to four peaks within 25 meV. These four peaks can be understood as resulting from alloying-induced coupling among the folded VCA states (intravalley coupling) with $k_x = (j/144)(2\pi/a)$ and $k_y = k_z = 0$, where a is the lattice constant of the VCA crystal and $j = 0,1,2,3$.

Because the coupling to states with higher j values diminishes quickly, we cannot obtain the dispersion curve of alloy states far away from the CBM. Nevertheless, we can estimate the Γ-valley effective mass of the alloy as $m(\Gamma, x = 0.5) = 0.0994m_0$, where m_0 is the free electron mass, which is very close to the VCA effective mass $m_{\mathrm{VCA}}(\Gamma,x = 0.5) = 0.103m_0$. Alternatively, one can use a smaller supercell—the 27 000-atom supercell, for instance—to obtain the dispersion curve of the alloy by applying the GMM using VCA states at different $\mathbf{k}$ points, which will be illustrated later for the effort to explore the global electronic structure of the alloy.

The result of Fig. 2(b) allows us to estimate the intrinsic broadening at the CBM due to intravalley scattering within the Γ valley, which can be viewed as inelastic scattering among the VCA states. The standard CPA theory for the alloy predicts, in the weak-scattering limit, a Lorentzian lineshape for all $\mathbf{k}$ states.[1] However, because the coupling to the states below the VCA (e.g., the valence band states) is very weak, the $A(\Gamma,E)$ spectrum is expected to be non-Lorentzian and asymmetric. For $E < 0$, we can assume $A(\Gamma,E) = 0$ for most practical purposes. For $E \geqslant 0$, a continuous spectrum of $A(\Gamma,E)$, equivalent to extrapolating to an infinite-size supercell, can be obtained by finding the envelop of the $j = 0$ to 3 peaks of Fig. 2(b). Because of the absence of the folded states along the k_y and k_z directions, the intensities of $j = 1$ to 3 should be approximately 3 times as strong as those of Fig. 2(b) if all three directions are included. We find that the spectral function can be described by a stretched exponential function:

$$A(\Gamma,E) = A_0 e^{-\alpha E^{\beta}}, \tag{9}$$

with $\alpha = 1.162$, $\beta = 0.4842$, and $A_0 = 0.5663\ (\mathrm{meV})^{-1}$, where E is in meV. The integrated intensity is 0.857 for the range of 25 meV measured from the CBM. The FWHM, which measures the alloying-induced intrinsic broadening of the band-edge state, is $\Delta_{\mathrm{CB}-\Gamma} = 0.34$ meV as a result of the intravalley coupling. Note that, in the standard VCA-based scattering treatment, there would be no alloy scattering at the

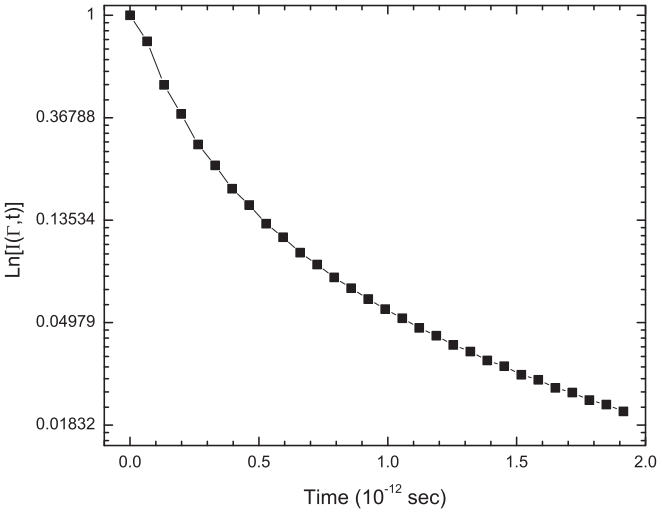

FIG. 3. Time decay of the Γ-like alloy state in the $Ga_{0.5}In_{0.5}P$ alloy.

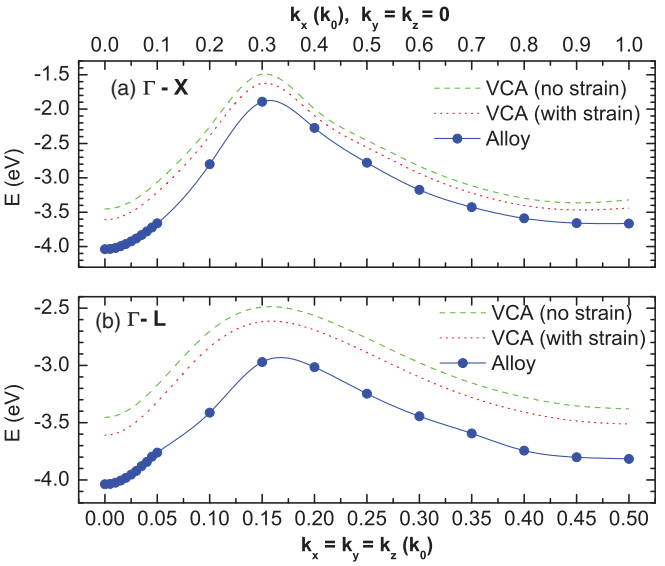

FIG. 4. (Color online) Effective dispersion curves of the $Ga_{0.5}In_{0.5}P$ alloy along the Γ-X and Γ-L directions, calculated using the generalized moment method (calculated discrete points interpolated by solid lines). The dashed and dotted curves are, respectively, the results of VCA without and with the inclusion of the strain term in the atomic pseudopotentials.

Γ point. However, in our case, the spectral width at the Γ point is finite, although small, which will result in a finite quasiparticle life time at the Γ point. Clearly $\Delta_{CB-\Gamma}$ is very different from Δ_{cf} in origin. We note that $\Delta_{CB-\Gamma}$ corresponds to an infinitely large alloy, whereas the energy fluctuation in the length scale of other coexisting physical mechanisms, such as excitonic effects or electron-phonon scattering, are more relevant in reality to the excitonic linewidth or transport.

We may use the formalism derived from single-site scattering theory to approximately describe the decay of the Γ-like state:[1]

$$I(k,t) = \left| \int_0^\infty dE e^{-iEt/\hbar} A(\mathbf{k},E) \right|^2 . \qquad (10)$$

Contrary to the ideal case,[1] the time dependence is nonexponential, as shown in Fig. 3, but the $1/e$ decay time, which may be considered as the scattering time $\tau_s(\mathbf{k})$, is found to be 0.21 ps for the Γ point. One could take this decay time as the lifetime of a VCA state that is viewed as a wave packet constructed by the alloy eigenstates within a small energy spread. After an average under electron thermal distribution (at different $\mathbf{k}$ points near Γ), τ_s is often used to estimate the electron mobility μ_e, which is simply $e\tau_s/m^*$ in the Drude model.[2] Note that this scattering time, which is also known as the "quasiparticle lifetime,"[1] is quite different from the real-carrier lifetime due to either radiative recombination with a hole or relaxation to defect or impurity states below the CB band edge. Here, the electron is scattered into a different state (e.g., in the Boltzmann equation), whereas for the real-carrier lifetime, the carrier is eliminated. In fact, the real-carrier lifetime is much longer in a high-quality alloy sample. For instance, the electron lifetime measured by radiative decay of the photoluminescence at low temperature (e.g., 1.5 K) is on the order of 200 ps for the $Ga_{0.5}In_{0.5}P$ alloy.[22]

B. Alloy states far from the band edge

Next, we apply the GMM to calculate the electronic "dispersion" relations along the two high-symmetry lines Γ-X and Γ-L of the BZ. Figure 4 shows the alloy "dispersion" curves for $Ga_{0.5}In_{0.5}P$, comparing with the results of VCA with and without the strain effect (i.e., the strain parameter $a_s \neq 0$ or $a_s = 0$ in the atomic pseudopotential). The three curves appear to have a similar shape, but the difference between the alloy and VCA can be more than 0.5 eV and is nonconstant throughout the BZ. The energy state on the alloy curve for a given $\mathbf{k}$ is determined from the peak position of the spectral function $A(\mathbf{k},E)$, using the 27 000-atom supercell.

The spectral function $A(\mathbf{k},E)$ at the band edge of a direct-band-gap alloy has been shown to be very sharp, as illustrated in Fig. 2(b). Figure 5 shows how $A(\mathbf{k},E)$ evolves along the Γ-X and Γ-L lines, computed using the 27 000-atom supercell and $m = 200\,000$. For those $\mathbf{k}$ points very close to the Γ point, for instance, $\mathbf{k} = 0.05\mathbf{k}_L$, the spectra show a single peak and its linewidth is dictated by the "spectral resolution" related to γ in Eq. (7). The peak position correctly gives the energy level on the dispersion curve, although the peak height is affected by the inadequate supercell size. For those $\mathbf{k}$ points slightly further away from the Γ point, for instance $\mathbf{k} = 0.10\mathbf{k}_L$, the coupling to the adjacent $\mathbf{k}$ points are apparent, even in the linear plot, indicating enhancement in "intravalley scattering." In general, the further away from the band edge is a VCA state, the broader the distribution of the VCA state is in the alloy energy spectrum. For the $\mathbf{k}$ points close to the highest-energy point of the dispersion curve, for instance $\mathbf{k} = 0.40\mathbf{k}_L$, the $\mathbf{k}$ VCA state is found to disperse into alloy states in a spectral range more than 0.5 eV. The peak height has reduced from $A_0 \sim 566$ eV^{-1} at Γ to $A_0 < 5$ eV^{-1} at $k = 0.4\mathbf{k}_L$, which means that the alloy state with the largest $\mathbf{k}$ component contains less than 1% of the $\mathbf{k}$ component. In a spectroscopy measurement, such an alloy effect will reflect in the reduction in the signal intensity and linewidth broadening. The detail depends on the type of measurement, which is beyond the scope of this work.

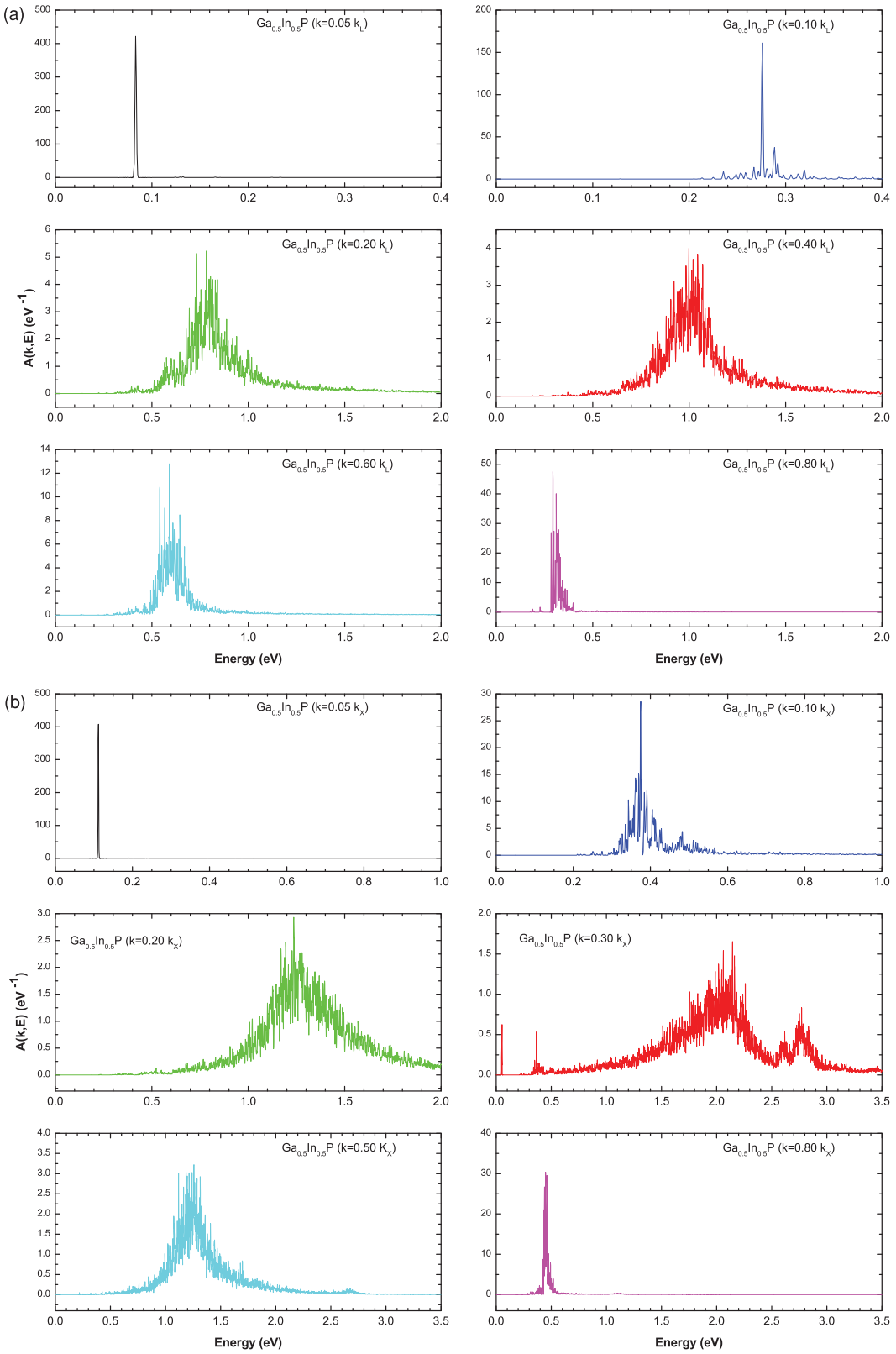

FIG. 5. (Color online) Spectral functions at various **k** points in the VCA Brillouin zone calculated for the $Ga_{0.5}In_{0.5}P$ alloy (a) for the (111) direction and (b) for the (100) direction. The energy reference is the conduction band minimum. A 27 000-atom supercell is used.

It is of particular interest to examine $A(\mathbf{k},E)$ at a critical point, because it provides a clearer picture for the intervalley and intravalley scattering than at a general **k** point. Figure 6 shows the spectral functions for the X and L point, calculated for all the VCA states belonging to different degenerate valleys X_1-X_3 and L_1-L_4. For the L-like alloy state and approximately 0.22 eV above the band edge, as shown in Fig. 6(a), the alloying effect is dominated by intervalley scattering, as indicated by

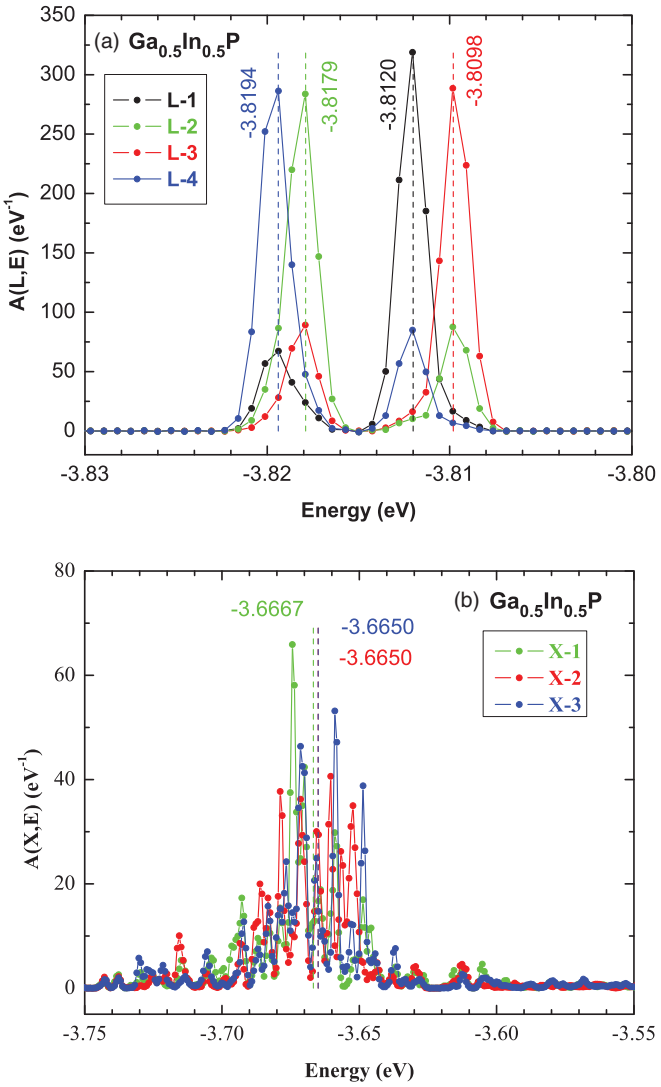

FIG. 6. (Color online) Spectral functions for the $Ga_{0.5}In_{0.5}P$ alloy calculated using the generalized moment method and corresponding to (a) four VCA L_1 states, showing the coupling due to the intervalley scatterings, and (b) three VCA X_1 states, showing more extensive decompositions of the VCA X_1 states among the alloy states centered around −3.66 eV. The positions of the X_1-like alloy states are estimated by performing weighted averaging over the alloy states. A 27 000-atom supercell is used.

the four separate peaks spread out in a range of ∼10 meV and derived from the four L valleys. For the X-like state approximatley 0.37 eV above the band edge, as shown in Fig. 6(b), there are apparently more alloy states involved, spreading out in a range greater than 40 meV, and one could not unambiguously identify three X-like peaks. The larger number of peaks for the X-like state, in contrast to the L-like state, could be understood as due to more significant intravalley scattering because, on the one hand, the X-like state is further away from the band edge and, on the other hand, in VCA, as shown in Fig. 4(a), the X point is not the local minimum along the Γ-X line, which leads to large number of states that are energetically degenerate with the X point and that have **k** vectors close to that of the X point.

From the alloy dispersion curves shown in Fig. 4, we can calculate the effective masses near the Γ point along both the Γ-X and Γ-L lines and even examine the possible anisotropy and nonparabolicity of the dispersion, which was not possible before. For reference, we find the VCA effective masses to be 0.103 and 0.106, respectively, for the [0,0,1] and [1,1,1] directions, and the nonparabolicity starts near 5% $\mathbf{k}_X$ or $\mathbf{k}_L$. The masses for the alloy are practically the same as the VCA results: 0.103 ± 0.001 and 0.106 ± 0.001 for the [0,0,1] and [1,1,1] directions, respectively, which means that the alloy band dispersion near the BZ center is very close to that of the VCA and is nearly isotropic, but with a rigid shift in energy from the VCA dispersion curves. Note also that the [0,0,1] effective mass agrees well with that estimated from the spectral function of the Γ point. We expect that the proper supercell size for computing the effective mass should be the similar to that for the band gap, because the states at different **k** points experience the same alloy configuration, so the energy difference between nearby **k** points is not as sensitive to the alloy configuration fluctuation as the band gap itself. In general, the higher-lying states tend to require larger supercells for achieving the same convergence as the band-edge state. However, one might not need to achieve the same convergence in practice because the higher-lying alloy states tend to suffer more alloy broadening, as is supported by evidence from optical spectroscopy measurements.

C. Indirect-band-gap alloy

Above we have discussed intra- and intervalley scattering when the conduction band X- and L-like states are far from the lowest band edge. We now investigate the alloying effects for the composition region that resembles an indirect band gap semiconductor using $x_{Ga} = 0.8$ as an example and focusing on the conduction band. The band structures have been calculated in three ways: (1) averaging over 50 configurations of the 3456-atom supercell, (2) average of two 27 648-atom supercells, and (3) one 27 000-atom supercell. The lowest CB state energies are found to differ by less than 4 meV (−3.7225, −3.7187, −3.7205 eV) among the three results, which suggests that they are adequately converged.

The first three CB states are found all having $A(\mathbf{k}_X, E_i) \sim 0.9$ (summing over the three X valleys). Thus, they can be understood as split X_1-like states due to intervalley scattering. However, the splittings are significantly larger for the 3456-atom supercell than for the larger supercells; for instance, 7.1 vs. 1.7 meV between the first two states, as shown in Fig. 7. This is another example showing the nonequivalency of the two approaches. One can envision that the intervalley splitting will diminish if the supercell size is increased further, which would indicate that a macroscopic alloy should have the zinc-blend symmetry on average. However, the observed supercell-size dependence of the intervalley splitting suggests that the impact of alloy scattering depends on the spatial extension of a physical property that is used for probing. For instance, an excitonic state in a semiconductor alloy could be viewed as a probe of the alloy fluctuation with an approximate probe size of the Bohr radius of the exciton that is about the size of the 27 000 atom supercell;[21] whereas a defect or an isoelectronic impurity state could be sensitive to the alloy fluctuation on

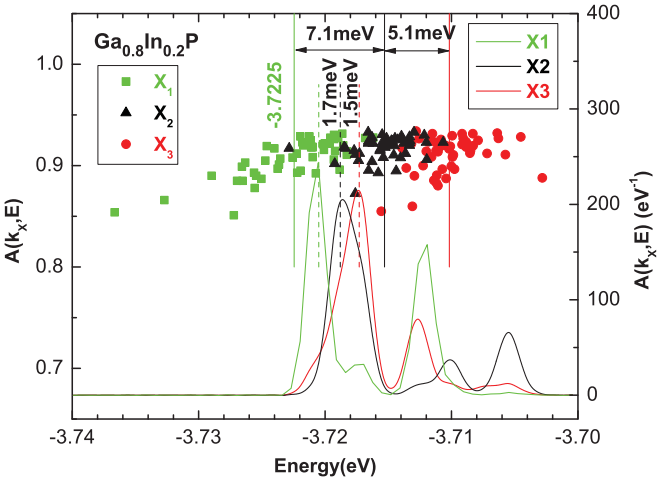

FIG. 7. (Color online) The effect of inter- and intravalley scatterings in the $Ga_{0.8}In_{0.2}P$ alloy. Left axis (discrete data points) gives the total X components of the three X_1-like alloy states for 50 random configurations of the 3456-atom supercell. The solid vertical lines indicate their average energies, and the splittings are caused by intervalley scattering. Right axis (continuous curves) gives the spectral functions for the three VCA X_1 states calculated using the generalized moment method and the 27 000-atom supercell. The dashed vertical lines indicate the positions of the three X_1-like alloy states in the alloy with the splitting caused by intervalley scattering. Additional peaks on the higher energy side are produced by intravalley scattering.

a substantially smaller scale. For instance, an N impurity in $Ga_xIn_{1-x}P$ can sense the Ga and In coordination change in its first nearest neighbors.[23]

The additional peaks (calculated by GMM) shown in Fig. 7 on the higher energy side of the X_1-like alloy states are alloy states corresponding to the VCA states with $\mathbf{k}$ vectors such as $(\pm 14/15,0,0)$ that couple with the X_1 states through intravalley scattering. There are a total of six of them in this group (although not all are resolved in this plot), spanning an interval of about 9 meV. In contrast to Fig. 6(b) where the X_1-like states are far from the band edge in the direct-composition region, the present indirect-composition region exhibits significantly weaker scattering (i.e., only $\mathbf{k}$ points that are close in energy are involved) for alloys states near the CBM in the alloy. However, the $A(\mathbf{k}_X, E)$ spectra shown in Fig. 7 indicate that intravalley scattering is in fact comparable with intervalley scattering.

IV. DISCUSSION

A. Alloy scattering theories within the VCA framework

For an alloy $A_xB_{1-x}C$, the perturbation potential is $\Delta V = V - V_0$, where V and V_0 are the total alloy and VCA potential, respectively. Assuming no lattice relaxation, the perturbation matrix element is often given as

$$|\langle \mathbf{k}'|\Delta V|\mathbf{k}\rangle|^2 \approx Nx(1-x)|\delta V_{AB}(\mathbf{k}',\mathbf{k})|^2, \qquad (11)$$

where $\delta V_{AB} = V_A - V_B$ (V_A and V_B are atomic potentials for atom A and B) and the matrix element $\delta V_{AB}(\mathbf{k}',\mathbf{k}) = \langle \mathbf{k}'|\delta V_{AB}|\mathbf{k}\rangle$. Note that Eq. (11) is valid only for $\mathbf{k}' \neq \mathbf{k}$, under the assumption that the two-body terms involving two atoms on different sites (A-A, B-B, and A-B) are all negligible.[24] The diagonal matrix element $\langle \mathbf{k}|\Delta V|\mathbf{k}\rangle = 0$ (although $\langle \mathbf{k}|\delta V_{AB}|\mathbf{k}\rangle \neq 0$) because $\langle \mathbf{k}|\Delta V|\mathbf{k}\rangle$ is simply the average of the potential fluctuation with respect to V_0, which perhaps provides the base for the common use of elastic scattering theory.

We first consider the theory for no lattice relaxation. In the context of the elastic scattering theory (within the first Born approximation), the square of the matrix element given by Eq. (11) is often related to the alloy scattering rate $1/\tau$ or the scattering-induced spectral broadening Δ.[8] Using this approach, because of the constraint imposed on elastic scattering, the linewidth Δ is zero for the nondegenerate Γ valley, and only intervalley scattering among degenerate valleys can yield nonzero Δ.[8]

Apparently, in this approach, the effect of inelastic intravalley scattering is not present. However, it has been shown in Sec. III C that inelastic intravalley scattering is actually quite significant for an indirect-band-gap alloy (Fig. 7), and in a direct-band-gap alloy it is the intravalley scattering that generates the finite linewidth $\Delta_{CB-\Gamma}$ for the Γ point (Fig. 2). Note that, in the literature dealing with the weak potential fluctuation, the spectral width of an alloy state is also given as $\Delta\mathbf{k} = \pi x(1-x)|\langle \mathbf{k}|\delta V_{AB}|\mathbf{k}\rangle|^2\rho(E)$ from Green's function theory, where $\rho(E)$ is the density of states.[2,8] Because $\rho(E)$ approaches zero for the Γ point, $\Delta(\Gamma)$ approaches zero, too,[2] although one could obtain a nonzero $\Delta(\Gamma)$ by introducing an imaginary part into E (termed "band tailing").[8]

Note that $\Delta_{CB-\Gamma}$ and $\Delta(\Gamma)$ are very different in nature. The former is the result of inelastic scattering whereas the latter is the result of elastic scattering. Also note that, in the alloy scattering discussion, "elastic" and "inelastic" scattering are not actually associated with the energy change of an alloy state, but rather with the coupling among the VCA states, either degenerate or nondegenerate, that is induced by the potential fluctuation.

With lattice relaxation, the diagonal term $\langle \mathbf{k}|\Delta V|\mathbf{k}\rangle$ becomes nonzero—typically a few hundred meV.[15] For the indirect-band-gap case considered above with $x = 0.8$, we have found that the diagonal and off-diagonal matrix elements among the X_1 states in fact have the same order of magnitude, $\langle \mathbf{k}'|\Delta V|\mathbf{k}\rangle \sim 0.1$– 0.2 eV. These results indicate that the conventional approach inappropriately neglects the inelastic scattering that is present even for alloys without lattice relaxation, and the treatment becomes more problematic when lattice relaxation is present.

B. An alloy transport theory not relying on a reference system?

Until now, we have followed the common practice in the literature to discuss alloy scattering in the framework of the VCA. We next point out a more fundamental issue of electronic transport theory within the framework of the VCA. Because of the use of the virtual-crystal structure as the reference, any deviation from the VCA will lead to nonzero scattering among the VCA states, which implies a reduction in carrier mobility. Obviously, an extreme example of a nonrandom distribution would be a structure with long-range order; for instance, a semiconductor superlattice.[25] For this case, it is not really meaningful to discuss "alloy scattering."

A more subtle situation is the well-studied partial long-range ordering that has often been observed in III-V semiconductor alloys, and in $Ga_xIn_{1-x}P$ in particular.[26] To some extent, it is still useful to use VCA states to characterize alloy states in a partially ordered structure.[15] However, it would be a nontrivial task to separate the effects of long-range ordering and alloy fluctuation if one attempts to calculate the scattering rate and the carrier mobility using the scattering matrix element based on the VCA. For a superlattice structure with imperfections such as atom interdiffusion, it would be more natural to use the ideal superlattice as the reference rather than the VCA. There is apparently some arbitrariness and nonuniqueness using either reference for evaluating the transport property. Furthermore, there is a disparity between electronic transport and electromagnetic wave propagation. For the latter, energy propagation can be calculated without relying on any reference system whether or not the medium is ordered or disordered. Therefore, a need exists to develop a theory that is independent of any reference system for electronic transport in a nonperiodic structure. The large-supercell direct calculation performed in the present work can play an important role in this regard.

V. SUMMARY

We compare two supposedly equivalent approaches to describe (semiconductor) alloys: (1) We used configuration averaging over many "appropriately sized" supercells versus using one "very large sized" representative supercell. We found that the specific size for either "appropriate size" or "very large size" depends on the problem of interest. For certain properties, such as the band gap, the two approaches are indeed capable of giving equivalent results. However, for others, such as properties related to alloy statistics, they are not at all equivalent.

We applied two techniques to analyze the global electronic structure of a semiconductor alloy system $Ga_xIn_{1-x}P$. A generalized moment method (GMM) is used to directly calculate the spectral function $A(\mathbf{k},E)$ of the alloy over the whole spectral range without having to explicitly calculate any alloy state, and this technique can deal with a very large system with >100 000 atoms (up to a few million atoms). The results can yield the band gap, dispersion curves (by projecting alloy states onto VCA states), and intrinsic alloy broadening that naturally includes both elastic and inelastic scatterings.

For a representative composition of $x = 0.5$ in the direct-band-gap region, we find that the intrinsic broadening for the Γ-like alloy state [i.e., the width of the spectral function $A(\Gamma,E)$] is non-Lorentzian and asymmetric with an estimated width $\Delta_{CB-\Gamma} = 0.34$ meV and a corresponding "quasiparticle" lifetime $\tau_s = 0.21$ ps. However, the width of the spectral function in the middle point of the BZ could be more than 0.5 eV. The alloy dispersion curve near the Γ point is nearly a rigidly shifted curve of the VCA with $m^* = 0.10m_0$. The intrinsic alloy broadening $\Delta_{CB-\Gamma}$ is fundamentally different from the energy fluctuation Δ_{cf} obtained by computing many "appropriately sized" alloy configurations and values for $\Delta(\Gamma)$ discussed in the literature. For a representative composition $x = 0.8$ in the indirect-band-gap region, we find that "inelastic" intravalley scattering, typically neglected in conventional alloy transport theory, is in fact of the same order of magnitude as "elastic" intervalley scattering; and the intervalley splittings obtained from configuration averaging over the "appropriately sized" supercells (~3500 atoms) is substantially larger than those from individual large supercells (~27 000 atoms).

It is satisfying to know that modern computation techniques like the one demonstrated here can directly calculate a system with size comparable to the extent of a physical interaction of interest (e.g., an exciton). This capability can open the way for detailed comparisons between theory and experiment regarding the experimentally observed statistical fluctuations in an alloy system.

We further discuss the need to develop an alloy transport theory that does not rely on the use of a reference system; for instance, the popular virtual crystal. We argue that the large-scale-supercell calculation can play an important role in such development.

ACKNOWLEDGMENTS

The work of Y. Zhang is supported partially by Charlotte Research Institute at UNC-Charlotte, and the work of L. W. Wang at LBNL is supported by the Director, Office of Science, Office of Basic Energy Science, Materials Science and Engineering Division, of the U.S. Department of Energy (DOE) under Contract No. DE-AC02-05CH11231. The work used the computational resources of NERSC at LBNL.

[1] H. Ehrenreich and L. M. Schwartz, *The Electronic Structure of Alloys* (Academic Press, New York, 1976), Vol. 31.
[2] A. B. Chen and A. Sher, *Semiconductor Alloys, Physics and Materials Engineering* (Plenum, New York, 1995).
[3] A. Zunger, S. H. Wei, L. G. Ferreira, and J. E. Bernard, Phys. Rev. Lett. **65**, 353 (1990).
[4] L. W. Wang, L. Bellaiche, S. H. Wei, and A. Zunger, Phys. Rev. Lett. **80**, 4725 (1998).
[5] P. Ernst, C. Geng, F. Scholz, H. Schweizer, Y. Zhang, and A. Mascarenhas, Appl. Phys. Lett. **67**, 2347 (1995).
[6] Y. Zhang, A. Mascarenhas, and L. W. Wang, Phys. Rev. B **63**, 201312R (2001).
[7] R. J. Lempert, K. C. Hass, and H. Ehrenreich, Phys. Rev. B **36**, 1111 (1987).
[8] C. H. Grein, S. Zollner, and M. Cardona, Phys. Rev. B **44**, 12761 (1991).
[9] S. Krishnamurthy, A. Sher, and A. B. Chen, Phys. Rev. B **33**, 1026 (1986).
[10] Y. Zhang, A. Mascarenhas, and L.-W. Wang, Phys. Rev. Lett. **101**, 036403 (2008).
[11] V. Popescu and A. Zunger, Phys. Rev. Lett. **104**, 236403 (2010).
[12] K. C. Hass, H. Ehrenreich, and B. Velický, Phys. Rev. B **27**, 1088 (1983).
[13] L.-W. Wang, J. Kim, and A. Zunger, Phys. Rev. B **59**, 5678 (1999).
[14] M. A. Steiner, L. Bhusal, J. F. Geisz, A. G. Norman, M. J. Romero, W. J. Olavarria, Y. Zhang, and A. Mascarenhas, J. Appl. Phys. **106**, 063525 (2009).

[15] Y. Zhang, A. Mascarenhas, and L.-W. Wang, Phys. Rev. B **78**, 235202 (2008).
[16] L. W. Wang, and A. Zunger, J. Chem. Phys. **100**, 2394 (1994).
[17] L.-W. Wang, Phys. Rev. B **49**, 10154 (1994).
[18] P. Keating, Phys. Rev. **145**, 637 (1966).
[19] Y. Zhang, A. Mascarenhas, and L. W. Wang, Phys. Rev. B **64**, 125207 (2001).
[20] Y. Zhang, A. Mascarenhas, S. Smith, J. F. Geisz, J. M. Olson, and M. Hanna, Phys. Rev. B **61**, 9910 (2000).
[21] K. K. Bajaj, Mater. Sci. Eng., R **34**, 59 (2001).
[22] P. Ernst, C. Geng, F. Scholz, and H. Schweizer, Phys. Status Solidi B **193**, 213 (1996).
[23] H. Mariette, J. A. Kash, D. J. Wolford, and A. Marbeuf, Phys. Rev. B **31**, 5217 (1985).
[24] G. L. Hall, Phys. Rev. **116**, 604 (1959).
[25] L. Esaki and R. Tsu, IBM Res. Dev. **14**, 61 (1970).
[26] A. Mascarenhas and Y. Zhang, in *Spontaneous Ordering in Semiconductor Alloys*, edited by A. Mascarenhas (Kluwer Academic/Plenum Publishers, New York, 2002), p. 283.